

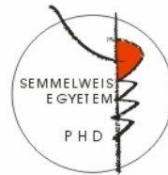
Molecular regulation of thyroid hormone activation

Ph.D. Thesis

Péter Egri

Semmelweis University

János Szentágothai Ph.D. School of Neuroscience



Tutor: Dr. Balázs Gereben, D.Sc.

Opponents: Dr. Endre Nagy, D.Sc.
Dr. Árpád Dobolyi, D.Sc.

Chairman of committee: Dr. Miklós Tóth, D.Sc.

Members of committee: Dr. Krisztina Kovács, D.Sc.
Dr. Andrea Tamás, Ph.D.

Budapest

2016

1. INTRODUCTION

Thyroid hormones (THs) are essential regulators of metabolism, neural development and brain function. Synaptogenesis, myelination, cell migration and developmental programs are fundamental TH-dependent functions. Hippocampal and cerebellar development is strongly affected by THs underlying the consequences of insufficient TH levels in motoric, cognitive and memory functions. THs are crucial regulators of the developmental program of sensory organs e.g. auditory system and retina. Therefore impaired TH signaling results in severely affected function of central nervous system (CNS) and perinatal hypothyroidism requires rapid supplementation of THs to avoid irreversible developmental deficits. THs have also major impact on the periphery; fat and liver metabolism, heart rate, muscle tone and the brown adipose (BAT), a crucial site of rodent and human neonate thermogenesis are under the control of THs.

The synthesis and secretion of THs from thyroid gland are controlled by the hypothalamo-pituitary-thyroid (HPT) axis. The axis is organized by thyrotropin releasing hormone (TRH) secreting neurons in the hypothalamic paraventricular nucleus, thyroid stimulating hormone (TSH, thyrotropin) synthesizing cells of the adenohypophysis and the thyroid gland itself. TSH stimulates both the release of THs from the thyroid gland and upregulates the required elements of TH synthesis. However, the HPT axis has obvious limitations in the spatiotemporal fine-tuning of TH action, especially in the brain. First, thyroid gland releases predominantly the stable prohormone, thyroxine (T_4) that is unable to bind to thyroid hormone nuclear receptors (TRs) that requires T_3 as a ligand. Second, the blood-brain, and the CSF-brain barrier have low permeability for T_3 therefore predominantly the transcriptionally inactive T_4 could be taken up by the brain parenchyma due to ligand specificity of the barrier forming cell-types. Therefore and as consequence the local TH action – especially in the brain – is established as the net effect of HPT axis regulated TH synthesis, TH transport, and local TH metabolism by deiodinase enzymes.

In the brain, TH activation – conversion of T_4 to T_3 – is carried out in glial cells by the type 2 deiodinase (D2) enzyme. Neurons are unable to generate T_3 themselves; they import glial-driven T_3 that affects the neuronal transcriptome. However, neurons are capable to control their intracellular active T_3 level via inactivation by the type 3 deiodinase (D3) enzyme.

Deiodinases are selenoproteins requiring the energy-dependent cotranslational incorporation of selenocysteine, also referred as the 21th amino acid.

Type 1 deiodinase (D1) is able to catalyze both the activation and inactivation of THs. However, the preferred substrate for D1 is the reverse T_3 (rT_3) that cannot be bound by TRs and D1 can efficiently generate T_3 only under hyperthyroid conditions. D1 is absent from human

central nervous system therefore is not involved in TH metabolism in the brain. D1 is a stable protein and not targeted by posttranslational modifications.

D2 is confined to catalyze the T_4 to T_3 conversion. D2 has three orders of magnitude lower K_M for T_4 than D1 therefore provides the primary T_4 activating capacity under euthyroid conditions. Unlike D1 and D3 that are localized in the plasma membrane, D2 homodimers are in stable retention in the endoplasmic reticulum (ER). The biochemical properties of D2 allow efficient TH activation that requires precise control ensured by a complex, multilevel regulatory system, as discussed below. Taking into account its exclusive expression as activating deiodinase in the CNS in human, D2 refers for the local T_3 generation in the brain. High D2 expression was also observed in muscle tissue and BAT.

D3 catalyzes the inactivation of THs. Biochemical characteristics provides the ability for D3 to inactivate T_4 directly to rT_3 or the conversion of T_3 to T_2 . D3 is expressed by neurons in the brain providing the opportunity to regulate their intracellular T_3 level.

The hypothalamic TH metabolism exerts major impact on the whole body via modulating the negative feedback regulation of HPT axis. Importantly, a significant portion of hypothalamic T_3 is generated by D2 expressed in special glial cells called tanycytes, located in the floor and the wall of the third ventricle. Therefore the dissection of mechanisms regulating D2 activity in these cells is of great importance. While several intracellular pathways were identified that regulate D2, upstream regulators of these cascades - especially in tanycytes - are largely unknown despite their pivotal role played in the modulation of feedback regulation of the HPT axis.

The *DIO2* promoter is under tight transcriptional control. Previous studies identified the cAMP/PKA signaling pathway as potent regulator of *DIO2* transcription. This mechanism was demonstrated to be involved in photoperiodic responses of the pineal gland, seasonal changes of hypothalamic T_3 generation and cold induction of BAT. However, the importance of cAMP/PKA pathway in the regulation of D2 in tanycytes and consequently its involvement in the modulation of HPT axis are poorly understood and available data are also limited on upstream factors regulating D2 via this pathway. *DIO2* promoter is also sensitive for NF- κ B that could underlie the pathogenesis of Low T_3 Syndrome when the increase of local T_3 production by infection in tanycytes suppresses the HPT axis and results hypothyroidism. TH level negatively affects *DIO2* transcription however it is not revealed whether it is a direct or indirect effect since a negative TRE could not be identified in *Dio2* promoter.

The most striking difference between the regulation of D2 and the other two deiodinases is represented by the short half-life of the D2 protein and its processing by the ubiquitin-proteasome system (UPS). This mechanism allows both rapid and reversible regulation of D2 activity via

conformational changes in the structure of D2 homodimers without degradation; furthermore ubiquitinated forms can undergo deubiquitination that results in the reactivation of the enzyme. Therefore the ubiquitinated D2 proteins provide a reserve pool allowing rapid induction of T₃ generation via deubiquitination without requiring *de novo* protein synthesis. D2 dimers in the ER are surrounded by complex ubiquitin-conjugating machinery including the ECS^{WSB1} and MARCH6 (TEB4) ligases and deubiquitinases USP33 (VDU1) and USP20 (VDU2). ECS^{WSB1} complex is built up from Cullin5 as backbone, Elongin B and C adaptor proteins, Skp1 and WSB1 F-box substrate recognition subunit. MARCH6 is a 14 transmembrane helix-containing protein involved in the ER-associated degradation. The ubiquitin-mediated inactivation of D2 is enhanced by T₄ that allows rapid regulation of T₃ generation. The region-specific expression of elements of this machinery could contribute to local adaptation of D2 activities in a T₄-dependent manner. This phenomenon was suggested to contribute the presence of distinct D2 regulation observed in different brain regions, e.g. TH regulation is homeostatic in the cortex, while not in the hypothalamus where integrates specific signals to modulate the HPT axis.

The UPS is constituted by two systems: the ubiquitin conjugation and degradation in the proteasome. The small ubiquitin protein is activated by E1 enzyme, transferred to E2 ubiquitin conjugating enzyme that carries ubiquitin moiety to the E3 ubiquitin ligase that binds the target protein and catalyzes the transfer of ubiquitin to a lysine of the substrate. The quantity of ubiquitin – and if it was synthesized – the quality of ubiquitin-chain fundamentally affect the further processing of substrates and only a subset – e.g. K48 lysine interlinked ubiquitin-chain tagged – of ubiquitinated proteins is degraded in the proteasome. The UPS has a broad range of biological functions including cell cycle and division, signaling and protein quality control etc. The degradation of ER-localized proteins contains an additional step: the ATP-dependent extraction from ER membrane before processed by the proteasome.

In conclusion, thyroid hormone activation by D2 is tightly controlled at multiple levels including transcriptional, pre- and posttranslational events and identification of these mechanisms are essential to reveal how TH economy is regulated in the brain and other tissues. Our studies were focused on i) hypothalamic mechanisms that regulate D2-mediated TH activation with consequences on the HPT axis, ii) and on better understanding of molecular and structural aspects of post-translational D2 regulation that could underlie the modulation of TH action in the hypothalamus and other tissues.

2. SPECIFIC AIMS

1. Novel mechanisms regulating the HPT axis via D2-mediated thyroid hormone activation
 - a) regulation of D2 transcription in the hypothalamus
 - b) interaction between thyroid hormone and pituitary adenylate cyclase activating polypeptide signaling

2. Involvement of MARCH6 ubiquitin ligase in the regulation of thyroid hormone activation
 - a) tissue distribution and transcriptional regulation of *MARCH6* gene
 - b) characterization of D2-MARCH6 interaction

3. Structural aspects of the ubiquitination of the D2 protein
 - a) combination of molecular elements required for the ubiquitin-mediated regulation of deiodinases
 - b) structural background of the recognition of D2 by ubiquitin ligases
 - c) importance of ER-membrane extraction in the reversible ubiquitin-mediated regulation of D2

3. MATERIALS AND METHODS

DNA constructs

Wild-type and cAMP response element mutant *DIO2* promoter luciferase reporter constructs was generated by PCR-based site-directed mutagenesis and cloned into pGL3-basic luciferase vector.

To analyze the expression pattern of *March6* in comparison with *Wsb1*, tissue samples were collected from adult male Wistar rats and total RNA was isolated using TRIzol method. After reverse transcription *March6*, *Wsb1* and housekeeping *Ppia* were amplified using intron-panning primers and amplicons were run in agarose gel.

3.5 kb 5' flanking region of human *MARCH6* gene was amplified from HEK-293T cells and cloned into pGL3-basic. Truncations were performed by digestion and religation.

FRET constructs were generated by subcloning D2, WSB1, MARCH6, and USP33 into fluorescent-protein fusion vectors. Mutations were inserted by PCR-based site-directed mutagenesis.

Chimeric deiodinases was generated on the strategy of inserting cassettes from D2 or site-directed mutagenesis. For FRET measurements these constructs were also subcloned into fluorescent-protein fusion vectors.

All constructs were confirmed by sequencing.

Cell culture and transfection

HEK-293T and HeLa cells were cultured in DMEM containing 10 % FBS and 1 % penicillin-streptomycin. Transfection was performed using Lipofectamine 2000 or Xtremegene HP reagents. All measurements or sample collecting were taken on the second day after transfection. Charcoal-stripped FBS was generated for 3,3',5-triiodo-thyronine (T_3) and thyroxine (T_4) treatments.

Reagents and treatments

T_3 and T_4 were dissolved in 40 mM NaOH. To generate charcoal-stripped serum, FBS was incubated with charcoal and dextran previously preincubated in Tris buffer. Tetracycline was dissolved in MQ water and used in 1 $\mu\text{g/ml}$ as final concentration. MG132 dimethyl sulfoxide (DMSO) and used in 2 μM final concentration. Eeyarestatin I (EERI) was dissolved in DMSO and used in 10 μM as final concentration. PACAP 1-38 was dissolved 0.9 % NaCl and used in 100 nM as final concentration. Forskolin was dissolved in DMSO and applied in 20 nM as final concentration.

Luciferase promoter assay

On the second day after transfection cells were washed ice-cold 1× PBS and collected in 1× Passive Lysis Buffer. Luciferase assay was carried out by using Dual-Luciferase Reporter Assay and Luminoskan Ascent equipment.

Quantitative PCR

Total RNA was isolated using TRIzol or RNeasy Lipid Tissue Mini Kit. RNA was transcribed using High-Capacity cDNA Reverse Transcription Kit, RNA and cDNA concentrations were determined by Qubit 2.0 fluorometric assay. TaqMan real-time PCR was applied for quantification of gene expression using TaqMan Fast Universal PCR Master Mix and TaqMan Gene Expression Assays. Reactions were run in ViiA™ 7 Real-Time PCR. Data were normalized by the geometric mean of *Gapdh* and *Hprt1* housekeeping genes for mouse tissue samples or *S18* for human cell lines. Gene expression was calculated by $2^{-\Delta\Delta C_t}$ method.

Western blot

Samples were harvested in Western lysis buffer with cOmplete™ Mini, EDTA-free protease inhibitor. Protein concentration was determined by Bradford method on Bio-Rad iMark Microplate Absorbance Reader. Samples were run in 4-20 % gradient or 10 % acrylamide/bis-acrylamide gel. FLAG-epitope was detected by M2 anti-FLAG monoclonal antibody used in 1:3000 dilution in 1× PBS and BM Chemiluminescence Western Blotting Kit.

Deiodinase assay

Tissue samples or cell pellet were sonicated in phosphate buffer. ^{125}I -labelled T_4 was purified on LH-20 Sephadex column. For D1 activity measurement assay mixture contained: 10 mM dithiothreitol, 100 000 CPM ^{125}I -labelled thyroxin, 1 μM thyroxin and total cell lysate in 300 μl as final reaction volume. For D2 activity measurement assay mixture contained: 20 mM dithiothreitol, 1 mM propylthiouracil, 100 nM T_3 , 100 000 CPM ^{125}I -labelled thyroxin, 100 nM thyroxin and total cell lysate in 300 μl as final volume. Assay was terminated by the addition of 200 μl normal horse serum and 100 μl trichloroacetic acid on ice. Samples were centrifuged on 13,000 rpm and supernatants were and measured using gamma counter.

Secreted alkaline phosphatase assay

Cells were cotransfected with the pSEAP2-Promoter plasmid. Media were collected on the day of cell treatment and measured using NovaBright Chemiluminescent SEAP Reporter Gene Assays and Luminoskan Ascent equipment.

Fluorescent resonance energy transfer (FRET)

Nikon A1R laser scanning microscope in virtual filter mode was used for FRET measurements applying acceptor photobleaching method: 453 nm argon laser for ECFP excitation with 464-500 nm detection range; 514 nm argon laser for EYFP excitation with 516-540 nm detection range; 561 nm DPSS laser for excitation of mCherry with 600-650 nm detection range. Cells with at least 80 % bleach efficiency were involved into analysis.

Animals and surgery

Animal experiments were performed in accordance with the legal requirements of the Animal Care and Use Committees of the Institute of Experimental Medicine (Hungarian Academy of Sciences, Budapest) following the European Communities Council Directive (2010/63/EU).

Stereotaxic surgery was used to insert 26-gauge stainless-steel guide cannula into the lateral ventricle of 8-week old male CD1 mice to the following coordinates: anteroposterior -0.2; lateral -1.0 and dorsoventral -2.0 from Bregma. After one week recovery 33-gauge stainless-steel internal cannula was connected to the guide cannula and 300 pmol PACAP 1-38 in 2 μ l artificial CSF (aCSF) or 2 μ l aCSF was injected into the lateral ventricle. Animals were sacrificed 4 hours after the treatment by decapitation, blood and tissue samples were collected.

Hypothyroid 8-week-old CD1 mice were generated by iodide-deficient chow and drinking water was supplemented with 0.1 % sodium perchlorate and 0.5 % methimazole for 3 weeks. Hyperthyroid mice were generated by administration of 15 μ g T₄/day/animal in 0.002 % BSA/PBS for 3 days.

Thyroid hormone measurement

Serum free T₃ and T₄ levels were measured using AccuLite CLIA microwells assays kit with Luminoskan Ascent luminometer and LIAISON® fT₃ and fT₄ assays with LIAISON® Analyzer.

TSH bioactivity measurement

CHO cells stably transfected with the human TSH receptor (CHO-TSHR) were plated 24-hours before the assay. Cells were preincubated in 90 μ l stimulation buffer for 30 minutes. 10 μ l serum samples were added to the cells and incubated for 1 hour followed by lysis in ethanol led to evaporate on 37 °C. Cells were collected in 50 μ l Lysis buffer. Lysates were processed for cAMP measurement using AlphaScreen cAMP Assay Kit and EnSpire® Multimode Plate Reader.

Immunohistochemistry

Mice were perfused transcardially with 40 ml 4 % paraformaldehyde dissolved in 0.1 M PB. The brains were removed and postfixed for 2 hours followed by cryoprotective immersion in 30 % sucrose in PBS overnight. 25 μ m thick coronal sections were cut using freezing microtome. Slices were permeabilized in 0.5 % Triton X-100 and 0.5 % H₂O₂ in PBS for 15 minutes and non-specific antibody binding was blocked by treatment in 2 % normal horse serum in PBS. Antibodies and sera were diluted in 2 % normal horse serum-containing PBS. PACAP receptor was detected by rabbit α PAC1R serum (generated by Dr. Shioda or Sigma, in 1:100 dilution), biotinylated donkey α rabbit-IgG (1:250), amplified by avidin-biotin complex and labelled by streptavidin-FITC conjugate (Jackson, 1:250). Vimentin was detected by goat α vimentin (Santa Cruz, 1:1500) and Alexa555 conjugated donkey α sheep-IgG (Thermo, 1:500). GFAP was detected by goat α GFAP (Santa Cruz, 1:500) and Alexa555 conjugated donkey α sheep-IgG (1:500).

Statistical analysis

Prism 3.0 and Statistica 8.0 software's were used for statistical analyzes. In brief, data were visualized as mean \pm SEM and for indication of significance level the following convention was used: *: p<0.05; **: p<0.01; ***: p<0.001. In general, two groups was compared by t-test, three or more samples were compared by the appropriate type of ANOVA and *post hoc* test.

4. RESULTS

4.1 Interaction between pituitary adenylate cyclase-activating polypeptide (PACAP) and thyroid hormone signaling

4.1.1 PACAP induces D2 expression via cAMP/PKA pathway

Previous studies revealed the set of intracellular cascades involved in the transcriptional regulation of D2. However, upstream factors involved in the regulation of D2 via these pathways are poorly characterized. Hypothalamus is a major target of PACAP action and PACAP overlaps the functions of TH therefore we tested whether PACAP could be involved in the regulation of TH metabolism in the hypothalamus via D2. In the first set of experiments the capability of PACAP to act on human *DIO2* transcription was tested using dual luciferase promoter assay. *DIO2* promoter activity was found to be induced by 100 nM PACAP-treatment in HEK-293T cells having demonstrated endogenous PAC1R PACAP receptor expression. To test whether this effect was transduced by cAMP/PKA second messenger system cAMP response element (CRE) mutant *DIO2* promoter was generated by site directed mutagenesis. NF- κ B subunit p65 was still able to induce the mutant promoter construct unlikely to PKA that was unable to upregulate demonstrating the specificity of the mutation for cAMP/PKA pathway. The effect of PACAP is completely abolished by the mutation of CRE indicating the induction by PACAP is transmitted by cAMP/PKA pathway.

4.1.2 Tanycytes express the PAC1R PACAP receptor

Immunohistochemical study was performed to identify cell-types and regions where PACAP is able to act on D2 transcription. Therefore the expression of PAC1R was investigated in astrocytes and hypothalamic tanycytes, representing the two major D2-expressing cell types in the brain. PAC1R immunoreactivity was found in tanycytes, the cells located on the floor and wall of the third ventricle referring for local T₃-generation in this region. This suggested that hypothalamic T₃ generation could be a target of PACAP. In contrast to tanycytes, PAC1R expression was absent in astrocytes in the hippocampus and cortex. However it should be noted that VPAC1 and 2 receptors with equal affinity for PACAP and vasoactive intestinal polypeptide (VIP) could be expressed by these cells and reactive astrocytes are found to express PAC1R.

4.1.3 PACAP affects the feedback and development of HPT axis

The previous experiments identified hypothalamic tanycytes as potential target of the PACAP-mediated regulation of D2 via cAMP second messenger. This mechanism was tested *in vivo* by 300 pmol intracerebroventricular PACAP administration to male CD1 mice. After 4-

hours of PACAP-treatment D2 activity in the mediobasal hypothalamus was elevated by 2.4-fold. To test whether the increased T_3 -generation affects the HPT axis on the level of TRH neurons tissue samples from the paraventricular nucleus were microdissected and subjected to quantitative PCR (qPCR). The *Trh* mRNA level was decreased by 45.89 % suggesting the increased local TH activation induced negative feedback of HPT axis. In parallel to *Trh*, the *Tshb* mRNA was suppressed by 23.30 % in the pituitary while *Dio2* was unaffected suggesting the indirect effect of PACAP in this region. TSH bioactivity was not decreased significantly after 4-hours of treatment however a tendency of decrease could be observed. The circulating free T_4 was also unaffected but it was expected taking into account the length of treatment.

The long term importance of PACAP in the regulation of HPT axis was assessed by investigating TH economy in PACAP-deficient mice. Serum free T_4 , T_3 and TSH bioactivity was decreased in heterozygous PACAP-deleted mice suggesting centrally uncompensated hypothyroidism. As a consequence of decreased TH availability, cortical and hippocampal D2 activities were elevated. In the mediobasal hypothalamus and pituitary – regions with crucial impact on the regulation of HPT axis – D2 activities were not affected significantly. Taking into account a tendency for increase in the mediobasal hypothalamus that was demonstrated to be involved in the suppression of HPT axis during infection and the antiinflammatory effect of PACAP; we tested whether an altered immune state could originate the observed phenotype. Therefore the concentrations of circulating inflammatory and antiinflammatory cytokines were measured however no difference could be found between genotypes. We speculated that the maturation and set-point of HPT axis could be altered by PACAP deletion. Therefore we assessed the TH economy of hypothalamus in 5-days old mice within the postnatal period when the setpoint of HPT axis is established. The periphery was hypothyroid indicated by decreased hepatic *Dio1* and increased *Thrb* level while hypothalamic *Dio3* expression was found to be upregulated. These data suggest that the formed setpoint of the HPT axis was fitted to low thyroid availability therefore the hypothyroid state was recognized as normal by TRH neurons and remained consequently uncompensated.

4.1.4 Thyroid hormones modulate *Adcyap1* (PACAP) gene transcription

In order to clarify whether THs affect PACAP signalization we studied the TH-mediated regulation of mouse *Adcyap1* gene encoding PACAP. The basal promoter activity of the 3 kb 5' flanking region of mouse *Adcyap1* gene was resistant to 0.1, 1, 10 and 100 nM T_3 concentration for 1, 3 and 5 hours of treatment measured by dual luciferase promoter assay. PACAP synthesis is positively regulated by cAMP/PKA pathway as demonstrated by cotransfection of constitutive active PKA. To test whether THs affect the cAMP/PKA-mediated induction of *Adcyap1* gene,

cells expressing the *Adcyap1* promoter-driven luciferase reporter were treated with 50 nM T₃ and/or 20 μM adenylate-cyclase agonist Forskolin in the presence or absence of mouse TRα. Simultaneous presence of TRα and T₃ interfere the cAMP-mediated induction of *Adcyap1* promoter indicating while PACAP synthesis is not regulated directly by THs however its activation could be modulated by TH environment.

The *in vivo* importance of this mechanism was assessed by qPCR-assisted measurement of *Adcyap1* expression in microdissected samples obtained from hypo- and hyperthyroid male CD1 mice. The investigation was focused on regions provides input for hypothalamic areas with crucial impact on HPT axis and energy homeostasis. In case of parabrachial nucleus suppressed *Adcyap1* expression was found in hyperthyroid mice while opposite regulation was revealed in the pituitary. However, in general *Adcyap1* expression was not affected by the altered TH status.

4.2 Characterization of the MARCH6 as D2 ubiquitin ligase

4.2.1 Expression profile of March6

The tissue distribution of *March6* mRNA ubiquitin ligase was studied in adult male Wistar rats in comparison with *Wsb1*. *March6* was found to be abundant in the pituitary, cortex, skeletal and cardiac muscle and kidney while nearly absent in liver and BAT, later showed abundant *Wsb1* expression. Interestingly, both ligases remained undetectable in the thyroid gland.

4.2.2 Characterization of the human MARCH6 promoter

To investigate the regulation of *MARCH6* expression the 3.5 kb 5' FR of human *MARCH6* gene was cloned and analyzed using TESS algorithm and TRANSFAC 6.0 database in order to predict transcription factor binding sites. Presumptive binding sites for important regulators of *DIO2* gene e.g. NF-κB and CREB were found in *MARCH6* promoter 5' proximal region adjacent to the transcription start site several SP1 sites were predicted. Using dual luciferase reporter assay the NF-κB and PKA were found to downregulate *MARCH6* promoter activity. The functional importance of SP1 sites was also demonstrated: deletion of the SP1 region resulted in 2-fold decrease of basal activity of the *MARCH6* promoter. Importantly, the *MARCH6* promoter was not sensitive for Sonic hedgehog (SHH) transcription factor GLI2 in this regulation *MARCH6* differs from *WSB1* ligase subunit that was shown to be induced by SHH.

4.2.3 Contribution of ubiquitination to the regulation of D2 in brown adipose tissue (BAT)

The PKA-mediated inhibition of *MARCH6* promoter suggested a mechanism how ubiquitination of D2 could be involved in cold-induced activation of T₃ generation in the BAT that process is governed by noradrenergic stimulus. To test this hypothesis, male CD1 mice were

transferred to 4 °C for 1, 2, 4, 6 and 9 hours and expression of genes involved in the ubiquitin-mediated regulation of D2 was measured by qPCR. *March6* expression was unaffected during cold stress while *Wsb1* showed elevated expression after the first hour and remained on induced level. *Usp33* deubiquitinase mRNA level was induced after 2 hours to 2-2.5-fold level compared to mice kept on thermoneutrality and the *Dio2* mRNA level was immediately induced to 10-25-fold while increased D2 activity followed the elevated transcript after 4 hours. *Ucp1* mRNA is found to be increased after 4-hours and increasing tendency was continued constantly.

In a reverse experimental design the response of ubiquitin-mediated regulation of D2 was tested after cold stress. Therefore male CD1 mice were kept on 4 °C for 8-hours, transferred to thermoneutrality at 30 °C and terminated after 0, 1, 2, 4 and 6 hours on thermoneutral temperature. Similarly to the previous experiment *March6* was unaffected by changing the ambient temperature. *Wsb1* mRNA level was rapidly felt to the control level after the end of cold stimulus. *Usp33* deubiquitinase expression showed rapid decrease however mRNA was still elevated after 6-hours. Kinetics of *Dio2* mRNA level was similar to that of *Usp33* however decrease in activity could be detected only after 6-hours. *Ucp1* expression was stable after 6-hours from the end of cold stimulus.

These data indicate a marginal role of ubiquitin conjugation in D2 induction during cold stress of BAT. The findings revealing the unexpected regulation of *Wsb1* need to be addressed by further investigations.

4.2.4 Topology of D2-MARCH6 interaction

Fluorescent resonance energy transfer (FRET) was performed to test and characterize the MARCH6-D2 interaction in living mammalian cells. The presence of interaction was tested for both termini both of MARCH6 and D2. Protein-protein interaction could be demonstrated between the RING-domain containing N-terminus of MARCH6 and the C-terminal globular domain of D2 ($E_{\text{FRET}} = 20.04 \pm 1.02\%$) that is located outside of the ER in the cytosol. In contrast, the C-terminus of MARCH6 did not interact either the N- or C-terminus of D2.

4.2.5 *Thyroid hormone-dependence of MARCH6-mediated regulation of D2*

We also tested whether MARCH6 could be involved in the TH-mediated inhibitory-loop of TH activation. The *MARCH6* promoter did not respond to 100 nM T₃ suggesting that on transcriptional level *MARCH6* is not affected by THs. However, the MARCH6-D2 interaction was increased by 39.17 % in 10 μM T₄ treatment indicating that MARCH6 is involved in the substrate-mediated downregulation of thyroid hormone activation by the ubiquitination of D2 enzyme.

4.2.6 *Construction of a 3-FRET approach to study parallel the interactions of D2 with the two E3-ligases*

It was shown before that hypothalamic tanycytes represent the only cell type in the brain that coexpresses D2 with both of its known E3 ligases, WSB1 and MARCH6. To study these interactions in living cells at the same time, we used a combination of three fluorophores in two FRET pairs that allowed the parallel detection of the interactions between D2 and WSB1 or MARCH6. We demonstrated that both ligases are involved in the T₄-dependent ubiquitination of D2 and contribute on a similar level in the regulation (55.55 % increase for MARCH6-D2 and 49.99 % for WSB1-D2 by 10 μM T₄).

4.3 Structural background of ubiquitination of deiodinases

4.3.1 *Molecular background of stability and ubiquitination of deiodinases*

To assess the minimal requirement for the short-half life and ubiquitination of deiodinases chimeric D1-D2 proteins were constructed. D1 was used as stable deiodinase background and ubiquitin-carrier lysines, instability-loop of D2 were inserted alone or in combinations. The protein was also directed into the ER by SEC62-fusion. Incorporation of one or two D2-specific lysines neither affect the ubiquitination nor stability however in combination with instability-loop led to decreased stability. Directing this double mutant chimera into the ER resulted in appearance of high molecular mass ubiquitinated forms and also reduced half-life. The ubiquitin-mediated regulation of chimeras was also tested via the inhibition of ubiquitin-proteasome system (UPS) by 2 μM MG132 proteasome inhibitor. Deiodinase activity of chimeras carrying alone or in combination the lysines and instability-loop was not affected by MG132 treatment indicating that these chimeras were not processed by UPS.

4.3.2 *Importance of D2-specific elements in the recognition by ubiquitin ligases*

The requirement of D2-specific elements for the recognition by ubiquitin ligases was studied by FRET measurements. We aimed to assess the criteria of interaction and identify which D2 ubiquitin ligases are involved in the processing of the ubiquitinated chimera. Similarly to the previous findings about stability, the ubiquitin-carrier lysines and loop or the localization in combination were insufficient for the recognition by both the WSB1 and MARCH6 ubiquitin ligases. Directing D1 into the ER by SEC62-fusion showed the same result. However, the combination of these elements and localization resulted in detectable FRET signal between the triple mutant chimera (carrying D2-specific lysines, instability-loop and targeted to the ER) and WSB1 ligase subunit however it was still insufficient for MARCH6. These data supports that the chimera contained lysines, instability-loop with ER-localization was processed by one of the D2-specific ubiquitin ligases. Additionally, difference in the recognition by WSB1 and MARCH6 suggests a distinct recognition motif inside D2 for these ubiquitin ligases.

4.3.3 *Effect of threonine/alanine polymorphism in D2 on the interaction with ubiquitin ligases*

The importance of the polymorphism in the first position (aa. 92) of the instability-loop in the ubiquitination of the human D2 protein was tested by FRET measurement. The basal interactions between D2 variants and WSB1 ligase subunit or MARCH6 ligase were not affected by T92A substitution. The T₄-mediated increase in the interaction between D2 and WSB1 ligase subunit was also found unaffected by T92A mutation. However D2-Ala⁹² and MARCH6 interaction was insensitive for the substrate-mediated induction of D2 ubiquitination. These results also support the previous findings that the two identified ubiquitin ligases of D2 recognize different binding surface and indicate altered processing of the polymorphic D2 variant by the UPS. Since polymorphic D2 is suggested to have a longer half-life *vs* wild-type, our finding revealed a mechanism that could contribute to this phenomenon.

4.3.4 *Relationship between deubiquitination and extraction of D2 from the ER*

Extraction of D2 from the ER membrane is a prerequisite of ubiquitination induced degradation of the D2 protein. Preliminary data revealed that the inhibition of extraction of D2 from the ER membrane did not result in increased D2 activity. To understand this contradiction, the interaction between the globular domains of D2 homodimers and the USP33 deubiquitinase was measured by FRET. Inhibition of the p97/VCP complex, responsible for ER extraction, by Eeyarestatin I (EERI) reduced the interaction between the D2 globular domains to the level measured in the presence of T4 and could not be further decreased by coaddition of EERI and

T₄. This suggested alterations in the ubiquitination-deubiquitination equilibrium of the D2 protein. To test this hypothesis, the interaction between D2 and USP33 was monitored by the inhibition of ubiquitination via MG132 and membrane extraction. A decreased USP33-D2 interaction could be observed when membrane extraction was abolished suggesting a lower deubiquitinating capacity that explains the lack of increased D2 activity under these conditions.

5. CONCLUSIONS

We identified PACAP as a potent activator of *DIO2* transcription via the cAMP/PKA signaling pathway. Among the D2-expressing cell types of the brain, tanycytes were found to express the PAC1R receptor. Intracerebroventricular PACAP administration increased D2 activity in the mediobasal hypothalamus that resulted in suppressed *Trh* in the PVN and decreased *Tshb* in the pituitary despite the proposed positive effect of PACAP on *Trh*. These findings revealed that PACAP regulates the HPT axis via D2 by a cAMP-dependent manner. PACAP was also found to be important in the maturation of HPT axis as PACAP-deficient mice showed remarkable alterations with centrally uncompensated hypothyroid phenotype. This could be caused by affected TH economy in the hypothalamus during the period when the set-point of HPT axis is formed.

March6 mRNA encoding an E3 ligase coexpressed with D2 in tanycytes was also found outside the hypothalamus in various rat tissues showing a tight overlap with *Wsb1* but both ligases were absent in the thyroid gland. Regulation of human *MARCH6* gene was studied focusing on factors with identified role in the transcriptional regulation of *DIO2*. This study demonstrated that potent activators of *DIO2* – PKA and NF- κ B pathways – downregulate the activity of *MARCH6* promoter providing an additional posttranslational mechanism to induce T₃-generation. To test this hypothesis *in vivo* the modulation of *March6* expression in BAT was measured by cold induction which governs cAMP/PKA cascade as downstream element of adrenergic stimulus. In contrast with *in vitro* data *March6* expression did not react to the upregulation of the cAMP/PKA cascade. Surprisingly, *Wsb1* expression showed a close correlation with cold stimulus suggesting an elevated turnover rate of D2 that could contribute to increased thyroid hormone activation via decreasing the pool of catalytically inactive D2 with an oxidized active center.

We demonstrated that the N-terminus of MARCH6 interacts with D2 in living mammalian cells. MARCH6 is also involved in the substrate-induced ubiquitination of D2 similarly to WSB1 ligase subunit while its expression is not targeted by THs. Constructing a 3-FRET system

allowed the parallel detection of interactions between D2 and its ubiquitin ligases, modeling the situation that can occur in tanycytes. We found an equal contribution of the two ligases in the process of T₄-mediated ubiquitination of D2. The deubiquitination of D2 was found to be functionally linked to the p97/VCP membrane extraction complex suggesting this step as rate limiting event in the degradation of D2.

Construction and stability measurement of D1-D2 chimeras revealed the combination of D2-specific elements as instability-loop, conserved lysines and ER localization is sufficient for the short half-life and ubiquitination of deiodinase proteins via ECS^{WSB1} ligase. The inability of MARCH6 to recognize the chimera containing these elements suggests a distinct recognition motif for D2 ubiquitin ligases. Similar difference was observed between the WSB1 ligase subunit and MARCH6 ligase in the recognition of T92A polymorph D2 protein that the mutation interferes with the substrate-induced increase in MARCH6 recognition. Our study also demonstrated a mechanism how the stability of D2 could be affected by the T92A polymorphism.

Our results contribute to the deeper understanding of the molecular regulation of TH activation and its functional impact on the modulation of the HPT axis.

6. PUBLICATION LIST

6.1 List of publications the thesis is based on

1. Zavacki AM, Arrojo E Drigo R, Freitas BC, Chung M, Harney JW, **Egri P**, Wittmann G, Fekete C, Gereben B, Bianco AC (2009)
The E3 ubiquitin ligase *TEB4* mediates degradation of type 2 iodothyronine deiodinase.
Mol Cell Biol 29(19):5339-47.
2. Arrojo E Drigo R*, **Egri P***, Jo S, Gereben B, Bianco AC (2013)
The type II deiodinase is retrotranslocated to the cytoplasm and proteasomes via p97/Atx3 complex
Mol Endocrinol 27(12):2105-15.
*equally contributed
3. **Egri P** and Gereben B (2014)
Minimal requirements for ubiquitination-mediated regulation of thyroid hormone activation
J Mol Endocrinol 53(2):217-26.
4. **Egri P**, Fekete C, Dénes Á, Reglódi D, Hashimoto H, Fülöp BD and Gereben B (2016)
Pituitary adenylate cyclase-activating polypeptide (PACAP) regulates the hypothalamo-pituitary-thyroid (HPT) axis via type 2 deiodinase in male mice
Endocrinology Epub 2016 Apr 5:en20161043.

6.2 Other publications

1. Christoffolete MA, Doleschall M, **Egri P**, Liposits Z, Zavacki AM, Bianco AC, Gereben B (2010)
Regulation of thyroid hormone activation via the liver X-receptor/retinoid X-receptor pathway
J Endocrinol 205(2):179-86.
2. Freitas BC, Gereben B, Castillo M, Kalló I, Zeöld A, **Egri P**, Liposits Z, Zavacki AM, Maciel RM, Jo S, Singru P, Sanchez E, Lechan RM, Bianco AC (2010)
Paracrine signaling by glial cell-derived triiodothyronine activates neuronal gene expression in the rodent brain and human cells
J Clin Invest 120(6):2206-17.
3. Schéle E, Fekete C, **Egri P**, Füzesi T, Palkovits M, Keller É, Liposits Z, Gereben B, Karlsson-Lindahl L, Shao R, Jansson JO (2012)
Interleukin-6 receptor α is co-localised with melanin-concentrating hormone in human and mouse hypothalamus
J Neuroendocrinol 24(6):930-43.
4. McAninch EA, Jo S, Preite NZ, Farkas E, Mohácsik P, Fekete C, **Egri P**, Gereben B, Li Y, Deng Y, Patti ME, Zevenbergen C, Peeters RP, Mash DC, Bianco AC (2015)
Prevalent polymorphism in thyroid hormone-activating enzyme leaves a genetic fingerprint that underlies associated clinical syndromes
J Clin Endocrinol Metab 100(3):920-33.

5. Jansen SW, Akintola AA, Roelfsema F, van der Spoel E, Cobbaert CM, Ballieux BE, **Egri P**, Kvarta-Papp Z, Gereben B, Fekete C, Slagboom PE, van der Grond J, Demeneix BA, Pijl H, Westendorp RG, van Heemst D. (2015)
Human longevity is characterised by high thyroid stimulating hormone secretion without altered energy metabolism.
Sci Rep. 19;5:11525.
6. Kollár A, Kvarta-Papp Z, **Egri P**, Gereben B (2016)
Different Types of Luciferase Reporters Show Distinct Susceptibility to T3-Evoked Downregulation
Thyroid 26(1):179-82.

7. ACKNOWLEDGMENTS

I would like to thank my tutor, Dr. Balázs Gereben for his support and the opportunity to perform my doctoral work in his laboratory.

I am very grateful to Professor Zsolt Liposits, Head of the Laboratory of Endocrine Neurobiology.

Special thanks to Professor Dóra Reglődi for the support of collaborative work. I wish to thank to Dr. Seiji Shioda providing anti-PAC1R serum and Dr. Attila Patócs for his help with thyroid hormone measurements.

I am very thankful to László Barna, Dr. Márton Doleschall, Dr. Csaba Fekete, Dr. Miklós Sárvári and Dr. Anikó Zeöld for their valuable methodological and technical advices.

I wish to thank to Vivien Hársfalvi and Andrea Juhász for their excellent technical help.

